A System Architecture for Battery-free IoT Networks

Dayrene Frometa Fonseca[‡*], Borja Genoves Guzman[§], Domenico Giustiniano[‡] and Joerg Widmer[‡]
[‡] IMDEA Networks Institute, Leganes, 28918, Madrid, Spain
Emails: dayrene.frometa@imdea.org, domenico.giustiniano@imdea.org, joerg.widmer@imdea.org
[§] University of Virginia, Charlottesville, 22904, Virginia, USA
Email: rrc3wc@virginia.edu

***Abstract*—While much research effort has been invested in long-range and low-power uplink communication for battery-free IoT networks, current deployments lack a scalable bi-directional communication infrastructure for data collection and processing with battery-free devices. To fill this gap, we introduce LoW-Fi, a system architecture specifically designed to meet the requirements of battery-free IoT applications. We show the suitability of LoW-Fi for deploying monitoring systems for precision agriculture indoors. This sector is revolutionizing with the installation of smart greenhouses that require the constant monitoring of ambient parameters to ensure optimal conditions for the crops growth. Our system is implemented using commercial off-the-shelf devices, and it works at the intersection of WiFi and LiFi for downlink and RF backscatter for uplink, retaining the advantages of each technology and solving their practical limitations. We evaluate LoW-Fi performance in a real greenhouse, and the experimental results show that it can achieve an uplink (downlink) range of 45 m (70 m) with 0% BER. The aggregated data rate is up to 4.5 Mb/s.**

I. Introduction

It is expected that by the year 2025, 75 billion of Internet of Things (IoT) devices will be deployed to enable new applications for our daily lives (i.e., smart homes and offices) and to solve critical global issues such as the food shortages due to population growth and climate change (i.e., precision agriculture in greenhouses and vertical farms). Many of these IoT devices will be sensors and actuators that will increasingly rely on battery-free IoT tags to reduce the carbon footprint of IoT deployments [1]. Multiple sectors requiring battery-free IoT devices are proliferating nowadays, such as precision agriculture, Industry 4.0 or smart homes, and current communication technologies cannot fulfill their real needs. As an example, sensors used in precision agriculture i) are pre-programmed and provided with uplink communication only, ii) involve a high-cost and inflexible infrastructure due to cabling and dedicated devices, which leads to low density deployments of sensors, and then a low measurement accuracy, and iii) involve a high-maintenance cost in case of wireless devices, due to the labor and battery replacement costs [2].

However, providing ubiquitous network access to billions of battery-free IoT devices has proven to be challenging. Research in battery-free IoT has started with the development of Radio-Frequency (RF) backscatter technology, the de-facto method for uplink communication from IoT tags. The research community has developed ultra-low-power RF backscatter systems meeting the low-energy consumption required by battery-free IoT deployments [3]–[6]. The typical architecture of a battery-free RF backscatter system presents four network elements: (i) the Carrier Wave (CW) generator to generate the carrier signal, (ii) the battery-free IoT tag that modulates and reflects the carrier to convey data in the uplink, (iii) the edge device to decode the backscattered packets from the IoT tag, and (iv) the energy harvesting source (sun or light bulb depending on deployments) to provide energy to the IoT tag. Although RF signals could also be used for energy harvesting, typically light energy is preferred due to the much higher energy that it provides [3], [5], [7]–[9]. The result is that existing RF backscatter networks face practical issues, as the *extreme low energy budget of IoT devices, which limits the design of any protocol to regulate the transmission access*, and the *interference generated by many IoT tags* transmitting simultaneously in the same band.

Need for bidirectional communication. This calls for a system design providing bi-directional communication links to send the collected data and receive and process protocol instructions. However, a strong limitation of prior work is that downlink communication from the edge device to the battery-free IoT tags has received low attention. The typical downlink option is to use passive RF receivers (i.e., envelope detectors), providing *very low sensitivity and high susceptibility to external interference*. This approach reduces the communication range of passive RF links, and causes *asymmetry in the network deployments* [6], further stressing the challenges for their integration with uplink solutions achieving larger communication ranges [3]. However, bi-directionality is essential for IoT applications that require not only receiving data from pre-programmed sensors [10], [11], but also sending processing instructions or control messages to implement net-

This work has been partially funded by European Union's Horizon 2020 Marie Sklodowska Curie ENLIGHT'EM project (814215), and in part by the project RISC-6G, reference TSI-063000-2021-59, granted by the Ministry of Economic Affairs and Digital Transformation and the European Union-NextGenerationEU through the UNICO-5G R&D Program of the Spanish Recovery, Transformation and Resilience Plan. The work of B. Genoves has been supported by the European Union (101061853).

work protocols. Moreover, the flexibility of triggering sensing tasks when really required will reduce RF interference and save energy at the battery-free IoT devices.

The pervasive deployment of LED-based lighting in greenhouses and vertical farms means a great opportunity to exploit it as communication devices too, without the need to deploy dedicated infrastructure [2]. Indeed, Light-Fidelity (LiFi) technology has recently started to be considered as an alternative to provide downlink access to battery-free IoT tags [3], [12]. However, current LiFi systems are not ready to be used as an access technology in real IoT deployments since they *lack an efficient backhaul solution* to connect the LiFi access points (APs) to the Internet [3], [12].

In this paper, we address the challenge of designing a bi-directional network architecture that meets the requirements of battery-free IoT applications, in particular for those where lighting infrastructure is easily available, as in greenhouse applications. Our system, represented in Fig. 3, is called LiFi over WiFi (LoW-Fi) and takes the best complementary features from existing technologies to enable the massive deployment of battery-free IoT tags.

The main contributions of this paper are as follow:

- We design and implement the first bi-directional network architecture that effectively integrates RF backscatter and passive LiFi technologies for battery-free IoT deployments. Our solution solves the individual limitations of RF backscatter and passive LiFi, providing reliable and scalable communication links.
- We design and implement the first WiFi-based backhaul solution enabling long-range simultaneous transmissions from an edge device to several LiFi APs. The proposed solution is suitable for low-data rate IoT communication, and it is standard-compliant with WiFi routers. It allows controlling subcarriers of the Orthogonal Frequency Division Multiplexing (OFDM) modulation of legacy WiFi standards without the need to use the Orthogonal Frequency Division Multiple Access (OFDMA) modulation of more recent standards.
- We design and implement the first LiFi AP that performs low-power and low-complexity Cross Technology Communication (CTC) conversion from WiFi to LiFi.
- We deploy and test our system in a real smart greenhouse. We show that LoW-Fi provides reliable communication links to the IoT tags, achieving a communication range of 45 m (70 m) in downlink (uplink) with a 0 % bit error rate (BER) and using around 15 dB less transmit power than the state-of-the-art solutions [3], [5], [6], [12].

II. Background on Battery-Free IoT Netwoks

In this section, we briefly review the necessary background on using RF backscatter for the *uplink* of battery-free IoT networks and the current efforts in the LiFi-based *downlink*.

A. Uplink based on RF backscatter

Current commercial wireless chipsets for active RF technologies include power-hungry radios to locally generate the RF signal. For instance, low-power WiFi chipsets for IoT applications consume at least 900 mW for transmission.[1] For a WiFi packet duration of 90 μs (20MHz, IEEE 802.11n, MCS0 with BPSK, coding rate 1/2, and 10 bytes), the consumption per packet transmission is about 81 μJ. Differently, in RF backscatter systems, the IoT tags do not actively generate the RF signals transmitted in the uplink. Instead, they exploit environmental RF signals and control the reflection coefficients to modulate them and convey data to the edge device. In comparison to active RF technologies, a commercial RF backscatter device consumes as little as 0.298 nJ/bit at a rate of 360 kb/s [11], resulting in a consumption of 23.84 nJ to send 10 bytes of data, which is more than 3000 times smaller than with an active WiFi radio. This extremely low-power consumption of RF backscatter allows allocating most of the harvested energy to sensing and computing tasks, which motivates the choice of RF backscatter as uplink technology for battery-free networks.

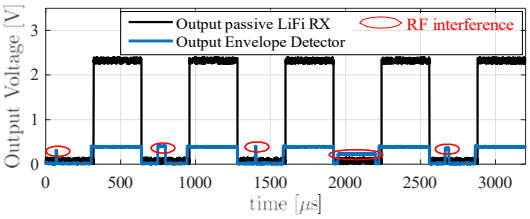

Fig. 1: Comparison between the output signals of a passive LiFi receiver and an RF envelope detector, both located at 1 m from the corresponding transmitter in an office environment.

B. Downlink based on LiFi

LiFi technology has attracted attention for downlink communications in battery-free IoT networks [3], [12]. This is because i) it allows reusing the lighting infrastructure to provide the battery-free IoT tags with both energy and communication, significantly reducing infrastructure costs; and ii) it enables the deployment of passive LiFi receivers that can address the ultra-low-energy constraints of battery-free IoT devices in the downlink and are more robust against external interference than RF envelope detectors, as we experimentally demonstrate in Fig. 1. As observed, the passive LiFi receiver is resilient to external interference and can thus provide lower BER, fewer false triggers, and, consequently, larger energy savings.

III. Challenges and Proposed Architecture

In this section, we study the limitations of current approaches to deploy battery-free IoT networks and motivate the solution proposed in this work for applications such as greenhouses where artificial light is already present.

A. Challenges

The traditional architecture choice for providing uplink communication through RF backscatter consists already of four network elements and the need to deploy a dedicated and dense infrastructure of CW generators [5], which increases

[1]See, e.g., ESP32-C3 Series Espressif and Telit WE866C3-P.

TABLE I: Backhaul solutions for multi-cell LiFi networks (NC: non commercial solution for LiFi backhauling)

	Technology	Installation Complexity	Range	Flexibility	HW Cost
Wired	Ethernet	High	Large	Low	~60 € + cabling costs [19]
	Optical fiber	Very high	Large	Low	
	PLC	High	Large	Medium	
Wireless	OWC	Medium	Short (<10m)	Low (LoS required)	NC
	RF (WiFi)	Low	Medium (<50m)	High	NC
	Our solution	Low	Large (>100m)	High	~7 € (COTS components)

the deployment costs. Therefore, it is undesirable to introduce additional separate elements to provide downlink communication.

For battery-free IoT applications where artificial light is present, the downlink can be provided with passive LiFi, whose architecture approach consists of (i) the LiFi transmitter to provide the battery-free devices with data and energy and (ii) the IoT tags equipped with a passive LiFi receiver to harvest energy from the light and decode the downlink data [3]. However, *there is not an efficient solution for the backhaul links from the edge device to the deployed LiFi APs* [3], [12], and current LiFi standards indeed acknowledge this issue [13]. In fact, current backhaul solutions for LiFi systems (e.g., Ethernet [14], power-line communication (PLC) [15], optical fiber [16], optical wireless communications [17], [18]) do not satisfy the requirements to enable LiFi as an access technology for battery-free IoT applications, since they cannot provide at the same time low complexity, large range, high flexibility for reconfigurable networks, and low cost for dense deployments of LiFi APs, as shown in Table I.

A trivial approach to provide the backhaul links in a LiFi network could be using WiFi chipsets at both the edge device and each LiFi AP. However, in this way, only one LiFi AP can access the channel at a time (simultaneous transmissions in the downlink are not possible), and decoding such large bandwidth reduces the communication range due to the noise power increase. Furthermore, adopting a WiFi chipset on each LiFi AP would increase the computational complexity, energy consumption, and time required to convert from WiFi to LiFi (i.e., WiFi packets must be fully decoded and then forwarded in the LiFi link).

B. Proposed architecture

As shown in Fig. 3, the proposed bi-directional network architecture consists of three network elements: LoW-Fi edge device, LoW-Fi AP, and the IoT tag. Such a network can be used in different applications for the development of smart systems. For example, in smart homes and offices to connect IoT sensors (i.e., temperature, humidity, illumination) and actuators to an application server that optimally controls these environmental parameters. It can also be deployed in smart agri-food facilities (greenhouses and vertical farms) to implement a monitoring and control system for precision

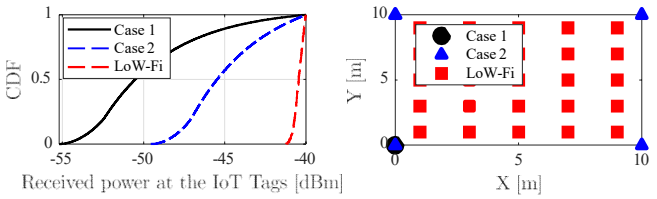

Fig. 2: On the left, the CDF of the received power at the IoT tags for different locations of CW generators. Cases 1 and 2 correspond to typical deployments of RF routers in offices and domestic environments, while LoW-Fi corresponds to the locations of CW generators proposed in this work. On the right, we show the location of CW generators for each case.

agriculture. And it can also enable applications for Industry 4.0, patient tracking in hospitals, or management of smart warehouses. For the sake of practicality, we test our system performance in a real smart greenhouse.

We propose a system that reduces the infrastructure costs and also ensures wide-area coverage by optimally allocating the required network components. To this end, we leverage the light fixtures distribution (already there for illumination purposes), to co-locate the RF carrier generators (i.e. CW generators) integrated into a single device (LiFi AP), as shown in Fig. 3. This approach eliminates the need for dedicated infrastructure and power outlets for the CW generators, while ensuring a homogeneous signal strength for the RF backscatter communication uplink, as depicted in Fig. 2. These results are obtained by assigning the same transmit power to the CW generators deployed in each case. Also, as in the state-of-the-art solutions [5], we have only one CW generator active at each time, associating each IoT tag with the nearest CW generator for a fair comparison. Finally, we also integrate our LoW-Fi edge device with WiFi routers already deployed in office and home environments, which further reduces the infrastructure and deployment costs.

LoW-Fi solves the lack of efficient communication links from the edge device to the LiFi APs with a novel RF-based backhaul solution that meets the requirements for battery-free IoT deployments. For the first time, we provide a standard-compliant WiFi router with capabilities to communicate, simultaneously, with multiple LiFi APs, further eliminating the need for dedicated network infrastructure.

To provide a scalable and long-range RF-based backhaul solution for battery-free LiFi systems, we exploit the Orthogonal Frequency Division Multiplexing (OFDM) of the WiFi standard (IEEE 802.11g/n) to associate individual WiFi subcarriers to *different* LiFi APs, providing as many simultaneous downlink transmissions as WiFi data subcarriers are. Also, since LiFi APs are listening to a single WiFi subcarrier, we can increase the communication range with respect to solutions demodulating the whole WiFi channel. In fact, considering Friis' transmission equation, for a fixed signal-to-noise ratio (SNR) value, the achieved distance is proportional to $1/B$, where B is the signal bandwidth.

To minimize computational complexity, energy consump-

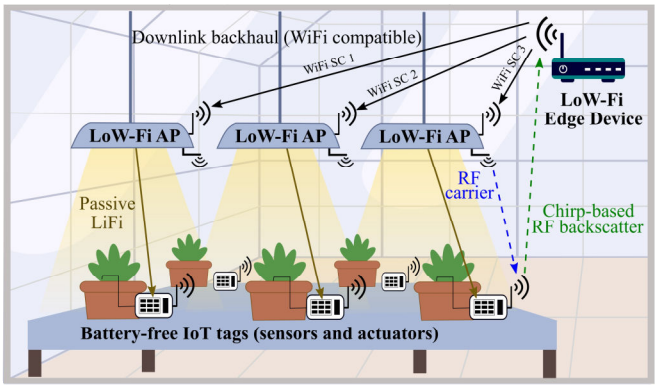

Fig. 3: System overview. In downlink (solid lines), the LoW-Fi edge device allocates subcarriers (SCs) to different LoW-Fi APs that send data to the IoT tags using LiFi. In uplink (dashed lines), the IoT tags use chirp-based RF backscatter exploiting the carrier wave generated by the LoW-Fi AP.

tion and latency at the LiFi APs, we implement a direct conversion technique from WiFi to LiFi, that only requires an RF front-end and a few Assembly instructions to work. Our LoW-Fi AP is the first bulb that performs a WiFi to LiFi CTC technique, receiving data with a simple RF front-end that matches its bandwidth and frequency with those of its assigned WiFi subcarrier. Whilst integrating multiple technologies, our solution is low cost and has very low complexity, which makes it suitable for multi-tag IoT deployments. To reduce the installation costs and boost the adoption of our LoW-Fi system in offices and home environments, our downlink backhaul solution is WiFi-compatible, meaning that we can use any commercial WiFi router as the edge device in our system.

In the next Section, we describe in details the scientific novelties and engineering contributions of the proposed architecture, and how the different network elements communicate among them.

IV. System Overview

Figure 3 presents the architecture of our LoW-Fi system, which can operate independently in uplink and downlink mode. For downlink, we use RF backhauling, transmitting data to the LiFi APs on WiFi subcarriers that we modulate at a rate of up to 62.5 kHz in the 2.4 GHz band. The battery-free devices can be placed a few meters away from the LiFi APs [3]. For the uplink, we cannot use WiFi subcarriers because the reverse process of synchronizing the IoT tags to achieve a WiFi packet of large bandwidth would be too complex and power-hungry [20]. We rather opt for chirp-based modulation in the 868 MHz band to guarantee a long range.

In our system, each element performs specific tasks during each operation mode, which are described in what follows.

LoW-Fi edge device. It is in charge of communicating with LoW-Fi APs in downlink and receiving data coming from IoT tags in uplink. For downlink communication, we exploit the OFDM modulation of IEEE 802.11g/n WiFi standards to implement an Amplitude Shift Keying (ASK)-OFDM modulation scheme per data subcarrier by reverse engineering a Commercial Off The Shelf (COTS) WiFi chipset. This provides an OFDM WiFi router with OFDMA capabilities. For uplink, we implement a chirp spread spectrum (CSS) demodulator to decode the data packets backscattered by the IoT tags.

LoW-Fi AP. The LoW-Fi AP includes a light bulb and an RF module. During downlink operation, it uses the RF module to receive and demodulate the ASK signal sent by the LoW-Fi edge device, directly converting it into a LiFi signal (intensity modulation) which is transmitted to the IoT tag using On-Off Keying (OOK) modulation. This conversion from RF to LiFi is carefully designed to keep low both complexity and latency at the LoW-Fi AP. The LoW-Fi AP also supports the uplink communication by generating (i) a LiFi baseband signal (a chirp similar to the one in [3], but implemented in this work inside the LiFi AP's firmware for taking into account constraints from real COTS devices), and (ii) an RF carrier wave signal for enabling low-power and long-range chirp-based RF backscatter. In this work, we exploit different spreading factors (SFs) associated with each LoW-Fi AP to enable concurrent transmissions in the uplink.

Battery-free IoT tags. The IoT tags in our system are equipped with (i) solar cells for light energy harvesting and data reception through the passive LiFi link and (ii) a passive RF transmitter that conveys data to the LoW-Fi edge device using a chirp-based RF backscatter technique. During downlink operation, the IoT tags demodulate the LiFi signals sent by the LoW-Fi AP, implementing an OOK demodulator to this end. During uplink operation, they receive baseband chirps from the LiFi link and use them to modulate the reflection coefficient of the antenna, reflecting the RF carrier wave signal that comes from the LoW-Fi AP with a frequency shift given by the frequency of the LiFi chirp [3].

V. System Design and Implementation

In what follows we present our system design and implementation for downlink and uplink operations, focusing on the edge device and the LoW-Fi AP, as for the battery-free IoT tag our design is based on the one proposed in [3].

A. Downlink

Figure 4 summarizes the main functionalities of the LoW-Fi system during downlink operation.

1) LoW-Fi Edge Device: During downlink operation, the LoW-Fi edge device embeds the data to different LoW-Fi APs on WiFi frames with an elaborated payload that, once transmitted over the air, emulates an M-ary Amplitude-shift keying (M-ASK) modulation scheme at each WiFi data subcarrier. We name it ASK-OFDMA. The specific tasks performed by the LoW-Fi edge device during downlink operation are depicted in Fig. 4. Specifically, it (i) associates WiFi data subcarriers with LoW-Fi APs to enable simultaneous transmissions in the downlink; (ii) maps M-ASK symbols to N-QAM symbols to perform an ASK-OFDMA modulation scheme with subcarrier granularity; (iii) finds the right payload

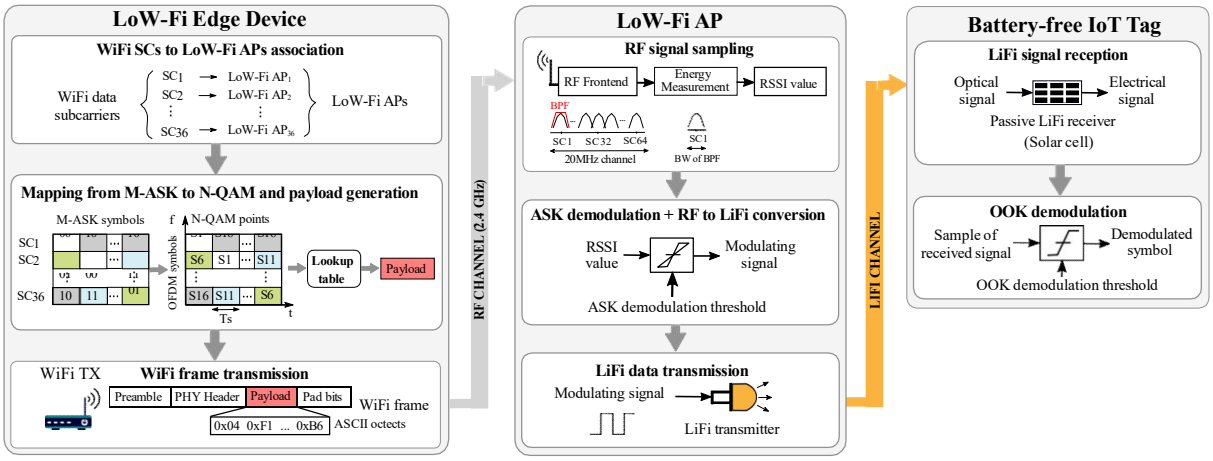

Fig. 4: Downlink operation of the proposed LoW-Fi system.

to embed the data for multiple LoW-Fi APs in a single WiFi packet transmission, which is done by checking a look-up table that results from reverse engineering the WiFi data encoding; and (iv) transmits the elaborated payload within a standard compliant WiFi frame through the air interface.

Proposed ASK-OFDMA modulation scheme. At the LoW-Fi edge device, we exploit the features of N-QAM to encode the data of each subcarrier with the amplitude of the QAM point we put on each of them. As represented in Fig. 4, and without loss of generality, we use the 64-QAM symbols summarized in Table II (i.e., S1, S6, S11, and S16) and place them accordingly among the data subcarriers comprising each WiFi OFDM symbol. We exploit the fact that a single OFDM symbol contains data for multiple subcarriers to convey data to different LoW-Fi APs simultaneously. We intentionally choose the 64-QAM points S1, S6, S11, and S16 for the mapping from M-ASK to N-QAM because they provide the largest Euclidean distance between them, so ensuring the most distinguishable ASK symbols. Fig. 4 shows an example of how the mapping from N-QAM to M-ASK works. For example, when using 2-ASK, to transmit the bit-stream '0 1, ... 1' to the LoW-Fi AP1, the WiFi transmitter places the 64-QAM symbols 'S1 S16, ... S16' on subcarrier 1 (SC_1) of consecutive OFDM symbols. Note that the maximum number of simultaneous transmissions with the proposed modulation scheme is limited to the number of data subcarriers within a WiFi OFDM symbol. Also, note that the maximum transmit rate is determined by the duration of the WiFi OFDM symbols (T_S in Fig. 4). Thus, considering the IEEE 802.11g/n standards, the maximum symbol rate we can afford is 250 ksymb/s (i.e., $1/T_S = 4\ \mu$s), which is sufficient for battery-free IoT applications. Finally, note that we can reduce this symbol rate by transmitting equal consecutive OFDM symbols. In this work, we configure the ASK-OFDMA transmitter to operate at three different data rates: 125 kb/s, 62.5 kb/s, and 31.25 kb/s, by sending 2, 4, and 8 consecutive identical OFDM symbols, respectively.

Implementation in COTS devices. We implement the WiFi transmitter of the LoW-Fi edge device using a COTS

TABLE II: Mapping between 64-QAM, 2-ASK, and 4-ASK symbols.

64-QAM symbols	2-ASK bit symbols	4-ASK bit symbols
S1 = $(1+j)/\sqrt{42}$	0	00
S6 = $(3+3j)/\sqrt{42}$	-	01
S11 = $(5+5j)/\sqrt{42}$	-	11
S16 = $(7+7j)/\sqrt{42}$	1	10

WiFi chipset (i.e., Atheros AR9285) integrated into an Intel NUC. We use MATLAB to reverse engineering the WiFi data encoding and derive a look-up table that maps the N-QAM symbols to be transmitted on each subcarrier to a valid WiFi payload. We have experimentally shown that our reverse engineering technique allows sending any combination of the M-ASK symbols listed in Table II on a total of 36 data subcarriers. This provides an aggregated transmission data rate of 4.5 Mb/s using 2-ASK with up to 36 simultaneous downlink transmissions.

Since we embed data into the payload of a WiFi frame, the maximum number of transmitted M-ASK symbols is limited to the IEEE 802.11 payload size (i.e. 2304 bytes without aggregation), which in turn depends on the coding rate and N-QAM modulation used. For instance, when using 64-QAM modulation and a coding rate of 3/4 (MCS6, IEEE 802.11n), the maximum number of ASK symbols we can transmit to each LoW-Fi AP within a WiFi frame is 85. Finally, note that our downlink solution is compatible with any communication standard implementing OFDM (i.e., long-term evolution, 5G, etc.). To extend it to other standards, we need to reverse engineer the corresponding COTS devices to obtain the specific payloads that will allow us to control the signal amplitude of individual subcarriers once it is transmitted over the air.

2) LoW-Fi AP: We design the LoW-Fi AP to perform communication between two technologies, the first one (WiFi) operating in the 2.4 GHz band and the second one (LiFi) in the visible light spectrum. Our design seeks to minimize costs and energy consumption while providing low complexity, low

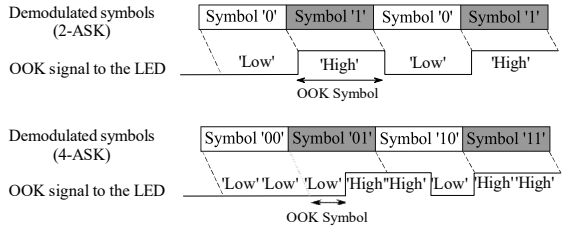

Fig. 5: 2-ASK and 4-ASK to OOK conversion at the LoW-Fi AP.

latency, and resilience to external interference. Fig. 4 shows the main functionalities of the LoW-Fi AP during downlink operation. As it can be observed, it is in charge of the following tasks: (i) sampling the received RF signal on the WiFi subcarrier it is associated with to retrieve Received Signal Strength Indicator (RSSI) values from it, (ii) performing the ASK demodulation and the conversion from RF to LiFi, and (iii) performing the LiFi transmission to the IoT tags.

RSSI readings and ASK demodulation. To decode the received packets, each LoW-Fi AP only needs to detect the amplitude variations on the data subcarrier it is associated with, which is done by measuring RSSI values as represented in Fig. 4. The retrieved RSSI values are used to recover the M-ASK symbols and to instantaneously modulate the light of the LED with an OOK modulation scheme.

RF to LiFi conversion. At the LoW-Fi AP, the demodulation of the received ASK signal and the generation of the OOK signal to modulate the light of the LED, are carefully combined to perform a direct conversion from RF to LiFi. Fig. 5 represents how our direct conversion technique works for both 2-ASK and 4-ASK. As can be observed, the shape of the OOK signal to the LED depends on the demodulated M-ASK symbols. When using 2-ASK, each time a new 2-ASK symbol is demodulated, the modulating signal to the LED is updated to 'High' if the demodulated symbol was '1' or to 'Low' if it was '0'. We follow a similar approach for 4-ASK, which, as depicted in Fig. 5, doubles the bit rate by halving the OOK symbol duration. Finally, note that our direct conversion technique significantly reduces the implementation complexity at the LoW-Fi AP by getting rid of any packet processing or buffering, which also minimizes the system delay, power consumption and hardware requirements when compared with legacy RF technologies (WiFi, ZigBee, etc.). More specifically, we design and implement the firmware of LoW-Fi AP to produce a minimum delay of 5 ns in the conversion from M-ASK to OOK.

Threshold for decoding. We implement a mechanism to dynamically adjust the ASK demodulation threshold at the LoW-Fi APs. It is executed each time a new frame is received and consists of using the RSSI readings corresponding to the WiFi preamble to derive the demodulation threshold. We notice that the WiFi preamble is a predefined sequence and it is the same for all the received frames as shown in Fig. 7. Based on this, we experimentally verify that the ratio between the RSSI readings of the WiFi preamble and the symbol of lowest energy (S1) does not change with the distance. We then

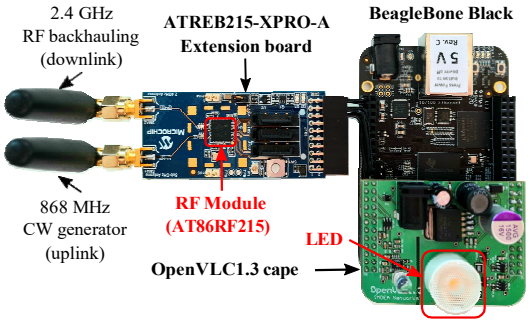

Fig. 6: Our prototype LoW-Fi AP.

define the demodulation threshold using such a ratio. Note that the proposed mechanism also provides resilience to external interference by dynamically adjusting the ASK demodulation threshold according to different interference levels.

Implementation. The prototype of our LoW-Fi AP is shown in Fig. 6. As can be observed, it mainly consists of three hardware components: (i) the AT86RF215 RF chipset to receive the ASK signals coming from the LoW-Fi edge device and to generate the carrier wave for uplink communications, (ii) the OpenVLC1.3 cape [21] to send LiFi data to the battery-free IoT tags and to generate the base-band chirps for uplink communications, and (iii) the BeagleBone Black (BBB) platform to control the previous hardware components and perform the direct conversion from RF to LiFi. Both the AT86RF215 chipset and the OpenVLC1.3 cape are directly connected to the General Purpose Input/Output (GPIO) pins of the BBB.

Experimental validation. Figure 7 shows experimental RSSI readings from three different LoW-Fi APs associated with the WiFi subcarriers 16, 17 and 18 of channel 6. It validates how the LoW-Fi edge device can send data to different LoW-Fi APs simultaneously by embedding all the data on a single WiFi frame. All the packets are transmitted using 2-ASK modulation, but a different data rate for each of them: 31.25 kb/s, 62.5 kb/s and 125 kb/s, corresponding to 10, 20 and 40 bits embedded within the LoW-Fi frames transmitted on the WiFi subcarriers 16, 17, and 18, respectively.

B. Uplink

The main functionalities of LoW-Fi system during uplink operation are shown in Fig. 8.

1) Design choices: Our uplink design is based on the RF backscatter solution introduced in [3], where the IoT tag mixes the CW signal from the RF source and the chirp baseband signal provided by the LiFi AP to create an uplink modulated signal based on the presence or absence of chirps. However, we substantially improve the system design in [3] as follows:

- We co-locate the CW generators with the deployed LoW-Fi APs to provide homogeneous signal strength of the carrier wave to the IoT tags and to reduce the infrastructure costs by avoiding the deployment of additional dedicated devices.
- We use chirps with a bandwidth of 125 kHz instead of 60 kHz, meeting the bandwidth of commercial chirp-based modulations [22]. Besides, we double the data rate by

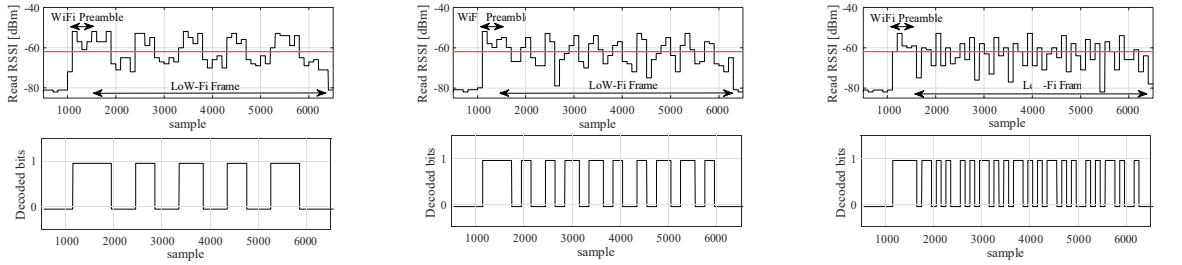

(a) 31.25 kb/s (10 symb/LoW-Fi frame) (b) 62.5 kb/s (20 symb/LoW-Fi frame) (c) 125 kb/s (40 symb/LoW-Fi frame)

Fig. 7: Frames decoded by three different LoW-Fi APs associated with the WiFi subcarriers 16, 17, and 18 of channel 6.

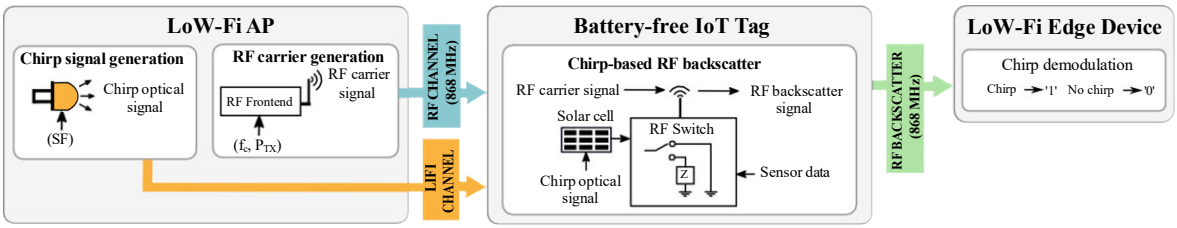

Fig. 8: Uplink operation of the proposed LoW-Fi system.

decreasing the symbol time according to $T_s = 2^{SF}/BW$ (SF indicates the spreading factor and BW the bandwidth);

- We implement the chirp baseband signal in the BBB firmware (instead of using an external input source as in [3]), which makes our solution ready to be deployed in real scenarios.

2) Implementation: We implement the functionalities of the LoW-Fi system components during uplink operation as follows.

LoW-Fi AP. We use the Sub-1 GHz RF chain of the AT86RF215 chipset in the LoW-Fi APs to generate the carrier wave signal required for RF backscatter uplink transmissions. To transmit the LiFi chirp we use the OpenVLC1.3 cape. These tasks are controlled by the Programmable Realtime Unit (PRU) 0 of the BBB through a highly precise Assembly code. The configuration parameters shown in Fig. 8 are the transmit power (P_{TX}), the frequency of the RF carrier wave (f_c), and the spreading factor (SF) of the chirp optical signal. They are informed by the LoW-Fi edge device to each LoW-Fi AP through the *resource allocation* message described in Section V-C.

Battery-free IoT Tag: We use the PassiveLiFi Tag introduced in [3]. Though we adopt the same modules and functionalities proposed by authors in [3], we use a new PCB design that integrates both the LiFi (receiver) and RF backscatter (transmitter) modules in a single PCB (shown in Fig. 9, left) to facilitate the deployment. As shown in Fig. 8, during uplink operation, the battery-free IoT tag mixes the RF carrier and the chirp optical signal (both generated by the infrastructure of the system) to produce and modulate the RF backscatter signal that is sent to the LoW-Fi edge device.

LoW-Fi edge device. During uplink operation, the LoW-Fi edge device acts as a chirp-based receiver to decode the backscattered packets coming from the IoT tags (cf. Fig. 8). It is implemented in the same Intel NUC platform we use as WiFi transmitter during downlink operation and the software defined radio USRP B210. For decoding the backscattered packets we modify the code of the LoRaSDR Pothos software [23] to detect the presence and absence of chirps with commercial-like compliant parameters.

C. Network operation

The proposed downlink and uplink LoW-Fi modes work in a time division duplexing manner.

Downlink time. The LoW-Fi edge device sends data to the IoT tags through the deployed LoW-Fi APs. The data frames transmitted in the downlink consist of an RF preamble, a LiFi preamble and a Data field. The last two are directly forwarded to the battery-free IoT devices following the conversion technique described in Section V-A2. In total, our system can communicate in the downlink with up to 36 LoW-Fi APs simultaneously, being limited by the number of WiFi data subcarriers within an OFDM symbol and by the reverse engineering approach [24]. If there is more than one IoT tag associated with a LoW-Fi AP, we follow a time division multiple access approach to give access to them.

Uplink time. The IoT tags transmit their data to the LoW-Fi edge device on their allocated time slots. In our LoW-Fi system, all the uplink transmissions are initiated by the LoW-Fi edge device, by sending a *resource allocation* message to the LoW-Fi AP serving the corresponding IoT tag. This message consists of an RF preamble and a command field indicating the SF, transmit power (P_{TX}), and central frequency (f_c) that should be used for the current uplink transmission. By carefully assigning different SFs and central frequencies among the LoW-Fi APs, our system can provide multiple simultaneous uplink transmissions with different SFs.

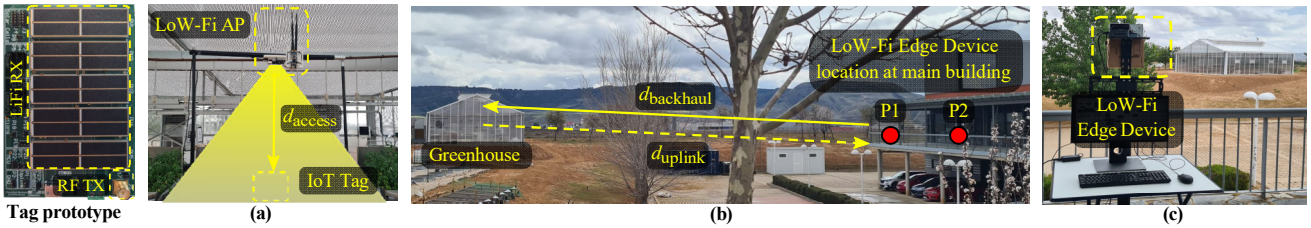

Fig. 9: Evaluation setup in a greenhouse, showing (on the left) the prototype of the IoT Tag, (a) the IoT Tag and LoW-Fi AP placements within the greenhouse, (b) campus of the research institute, and (c) the LoW-Fi edge device location outdoors.

Resource allocation. We implement a resource allocation algorithm at the LoW-Fi edge device that dynamically adjusts the parameters for uplink transmissions. It is updated each time a new uplink packet is received at the LoW-Fi edge device and uses the signal strength of such packet to optimize the configuration parameters shown in Fig. 8 (P_{TX}, f_c, and SF). In this way, our system parameters are dynamically adapted to new network conditions.

VI. Evaluation

In this section, we evaluate the communication performance of our LoW-Fi system in a real greenhouse and compare it with state-of-the-art solutions and WiFi technology.

A. Greenhouse application

LoW-Fi system presents many advantages for the implementation of cost-efficient and eco-friendly monitoring systems for precision agriculture in vertical farms and high-tech greenhouses. If we look at such agri-food facilities, we will find that the main components of our system are already there: LED lamps to ensure proper illumination conditions for the crops and a WiFi router for Internet connection. Thus, our system can retrofit the lighting infrastructure for LiFi communication purposes (implement our LoW-Fi AP) and reuse the WiFi router as our LoW-Fi edge device, which significantly reduces the infrastructure and deployment costs. On the other hand, our RF-based backhaul solution eliminates the need for dedicated devices and cabling to connect the IoT tags to the Internet. In fact, the experiment results show that our LoW-Fi edge device can reach the LoW-Fi APs within the greenhouse from the main building in Fig. 9, meaning that we can reuse the WiFi routers already deployed on the research institute to implement it. Finally, our LoW-Fi system enables the deployment of battery-free IoT tags to precisely monitor ambient parameters and actuate over other control systems within the greenhouse (i.e., irrigation, temperature control, etc.).

B. Evaluation setup and configuration parameters

Fig. 9 shows the evaluation scenario, which corresponds to a Reylux R9 greenhouse with dimensions 10x9 m [25]. We denote the backhaul distance (i.e. from LoW-Fi edge device to LoW-Fi AP) as d_{backhaul}, the access network distance (i.e. from LoW-Fi AP to IoT tag) as d_{access}, and the uplink distance (i.e. from IoT tag to LoW-Fi edge device) as d_{uplink}. For all the experiments (unless otherwise stated), we set d_{access} to 1.5 m.[2] Finally, note that, in this section, we focus on demonstrating the feasibility and communication performance of the proposed system architecture. We do not evaluate the performance of the algorithms implemented at the LoW-Fi edge device for the WiFi subcarrier to LoW-Fi APs mapping or for the resource allocation described in Section V-C because of their simplicity and space limitations.

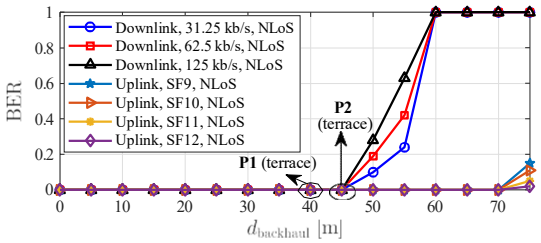

Fig. 10: BER under NLoS.

The transmit power and operation frequency of the LoW-Fi edge device and the carrier wave generator at the LoW-Fi APs are set to 14 dBm and 2.437 GHz (WiFi channel 6), and 13.4 dBm and 868 MHz, respectively. The bandwidth for the band-pass filter at the LoW-Fi AP is set to 320 kHz and tuned at the subcarrier center frequency to let pass only the signal on the subcarrier it is associated with. Finally, for the generated chirps, we use BW = 125 kHz and different SFs: from SF9 to SF12.

C. BER and range performance

We move the LoW-Fi edge device outside the greenhouse, as shown in Fig. 9. Note that there is non-line-of-sight (NLoS) between the LoW-Fi edge device and the rest of the system components placed within the greenhouse. Under this NLoS setup, we evaluate the following:

2-ASK downlink: Fig. 10 shows the BER during downlink operation for 2-ASK and NLoS. As shown, our downlink solution can provide a 0% BER for a distance of up 45 m for all the considered data rates. It also shows a 0% BER when placing the LoW-Fi edge device at P1 and P2 in Fig.9, which means that we could reuse WiFi routers located at the main building as the edge device for our LoW-Fi system.

4-ASK downlink: Fig. 11 gives us an insight on how the received RSSI values change with the distance when transmitting the 4-ASK symbols listed in Table II. Note that the RSSI regions must be re-defined for each distance, but they

[2]Note that the LiFi link does not include any errors for $d_{\text{access}} < 3$m [21].

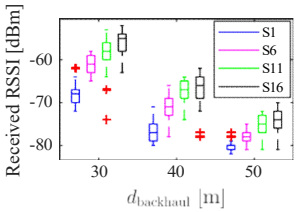

(a) 1st, 2nd and 3rd quartiles for 4-ASK RSSI readings.

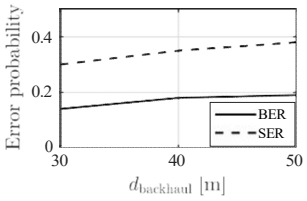

(b) SER and BER (Gray coding) results.

Fig. 11: 4-ASK performance under NLoS.

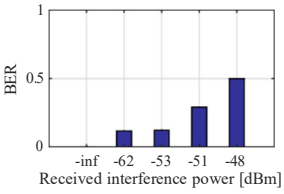

(a) BER for LoS and different interference levels.

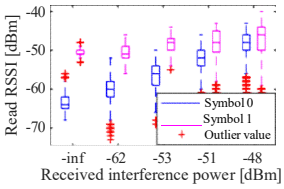

(b) 1st, 2nd and 3rd quartiles for 2-ASK RSSI readings.

Fig. 12: Downlink resilience to interference.

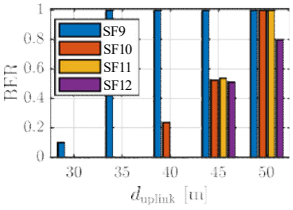

(a) One interfering source.

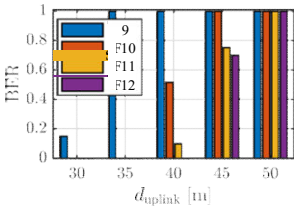

(b) Two interfering sources.

Fig. 13: Multi-tag deployment.

can be distinguished. BER values of around 15% are obtained for a distance of 30 m.[3]

Uplink: Fig. 10 also shows the BER during the uplink operation. Note that the uplink reaches 70 m with a 0% BER for all SFs and a BER lower than 10% for 75 m and the SFs 11 and 12.

From these results, we can conclude that LoW-Fi provides enough reliability and communication range to implement a monitoring system for precision agriculture in greenhouses. Also, note that deploying all the system components inside the greenhouse will provide a 0% BER both in downlink and uplink. Finally, notice that the illuminance conditions and the sampling rate of our system are higher and lower, respectively, than the ones considered in [3], which guarantees the self-sustainable operation of the IoT tag.

D. Downlink resilience to external interference

In this experiment, we evaluate the effectiveness of the mechanism proposed in Section V-A2 to make our backhaul downlink solution resilient to external interference by dynamically adjusting the ASK demodulation threshold at the LoW-Fi AP. We set d_{backhaul} = 10 m and place an interference source (continuously transmitting on the 2.4 GHz WiFi channel 6) in between the LoW-Fi edge device and the LoW-Fi AP. Then we measure the BER at the IoT tag under different interference levels. The minimum sensitivity for 64-QAM in IEEE 802.11n standard is -61 dBm (considering the whole 20 MHz band), which is in accordance with the interference levels created. Fig. 12 shows that low BER values are obtained up to a received interfering signal power of -51 dBm. Beyond this value, the RSSI values overlap when transmitting the symbols '0' and '1', which makes symbol decisions hard. By calculating the desired received power, we can compute the signal-to-interference power ratio (SIR) and conclude that LoW-Fi system works well for SIR larger than -11 dB when transmitting the 2-ASK symbols '0' and '1'.

E. Uplink resilience to inter-tag interference

In this experiment, we deploy multiple tags along the greenhouse. The IoT tags (i.e., Tag 1, Tag 2, and Tag 3) are separated by a distance of 1 m between them. To evaluate the effect of the inter-tag interference, we enable the tags' transmissions one by one until the three of them transmit simultaneously on the same channel but using different SFs. The interfering signals use SF11, SF11, SF12 and SF11 (SF11-12, SF11-12, SF10-12, SF10-11) for the case of one (two) interfering source(s), respectively. Fig. 13 shows the BER when decoding the packets transmitted by Tag 1 with different SFs and under different interference conditions. We observe that by increasing the number of interfering sources, we reduce the communication range achieved with each SF. For example, with SF11 and one interfering source (Fig. 13a), the system reaches up to 40 m with a 0% BER, while this distance is reduced to 35 m when two interference sources are enabled (Fig. 13b). These results show the possibility of concurrent uplink transmissions by allocating different SFs to the deployed IoT tags. Extending the system to four IoT tags allows for achieving an aggregated data rate of 458 b/s by allocating spreading factors from 9 to 12 among them.

F. Comparison with other systems

LoW-Fi vs. state-of-the-art architectural solutions. Table III compares our solution against state-of-the-art battery-free IoT systems in terms of their completeness, transmit power, and communication range. As shown, only LoW-Fi provides a complete bi-directional system based on non-dedicated infrastructure. Some systems are missing the backhaul links (i.e., PassiveLiFi) or rely on dedicated infrastructure (i.e., Multiscatter), which makes them expensive or impractical for real IoT deployments. Finally, note that LoW-Fi can achieve a larger range than other systems under NLoS (i.e., Multiscatter) but using around 15 dB less transmit power.

Regarding deployment costs, when compared to Multiscatter [5], our system halves the cost of the CW generators (~7 € vs. 14.77 €) and reduces in a 95% the number of reader devices required to cover certain area (i.e., a single LoW-Fi edge device can cover up to 8100 m^2, while Multiscatter

[3]Note that these BER values can be further decreased by invoking additional coding schemes. Also, for shorter distances, the BER will be lower.

TABLE III: Comparison with state-of-the-art battery-free IoT systems. (UL: Uplink, DL: Downlink)

System name	Bi-directional architecture	End-to-end range, NLoS
PassiveLiFi [3]	No (missing the backhaul link)	DL: 3.5 m (LiFi link); UL: 24 m @ 13.4 dBm
Multiscatter [5]	Yes (dedicated infrastructure)	DL: Not reported; UL: 33 m @ 28 dBm
HitchHike [6]	Yes (dedicated infrastructure)	DL: 1 m @ 30 dBm; UL: 16 m @ 30 dBm
LoW-Fi (our proposal)	Yes (non-dedicated infrastructure)	DL: 45 m @ 14 dBm; UL: 70 m @ 13.4 dBm

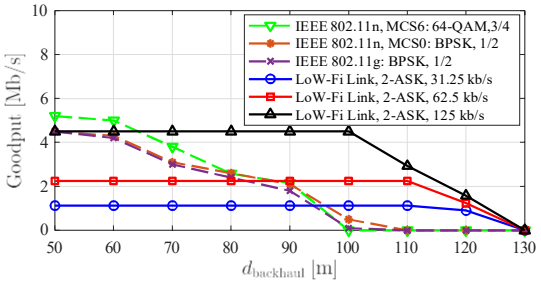

Fig. 14: Goodput and communication range comparison between LoW-Fi and traditional WiFi in a LoS outdoor scenario.

system needs 5 RXs to cover approximately 1/4 of that area (~2174 m^2) [5]. Finally, regarding the resilience to external interference, only our system presents such a characteristic by implementing the mechanism described in Section V-A2.

LoW-Fi vs WiFi. Now we demonstrate how the backhaul solution proposed in this work provides better communication range and scalability than the alternative of including a WiFi chipset at the LoW-Fi APs. We compare LoW-Fi only against WiFi, as WiFi's communication range is much larger than the ones provided by ZigBee or Bluetooth technologies. We have experimentally measured the link performance of WiFi and our LoW-Fi system in an outdoor line-of-sight (LoS) scenario. As expected, Figure 14 shows that LoW-Fi provides larger communication range than legacy WiFi standards. Also, for larger distances (more than 70 m), LoW-Fi outperforms WiFi in terms of aggregated goodput. Regarding scalability, note that WiFi, ZigBee, or Bluetooth technologies cannot provide simultaneous transmissions in a single channel, while LoW-Fi can achieve up to 36 simultaneous downlink transmissions using a single 20 MHz WiFi channel. Finally, in terms of power consumption, the RF receiver at the LoW-Fi APs consumes as low as 13.2 mW. This is one order of magnitude less consumption than a low-power WiFi chipset [26], which is around 200 mW for reception.

VII. Related work

We discuss here research works and technologies that are most related to our system.

Wireless technologies for battery-free IoT networks. Recent works on RF backscatter meet the requirements of ultra-low-power consumption and large-range communication from the battery-free IoT tags to the edge device [3], [5], [12]. However, they still face many practical limitations. Some works require a dense dedicated infrastructure of CW generators and RF readers or have high false detection of RF signals in downlink [5], which significantly increases the deployment costs and power consumption at the IoT tags. Other works have focused on addressing the high scalability requirement of IoT applications, enabling multiple simultaneous transmissions from the IoT devices to the edge device. Netscatter system [4] can provide hundreds of simultaneous uplink transmissions at the cost of battery-powered IoT devices, which is not an option when considering the imminent deployment of billions of them [1]. Moreover, the edge device in Netscatter system cannot be implemented in COTS devices, which limits its use in real IoT deployments. As shown through this paper, LoW-Fi solves the limitations mentioned above.

Backhauling for battery-free LiFi systems. For the downlink communication, recent works have proven that passive LiFi provides better communication performance than a passive RF receiver (envelope detector) [3], [12]. However, these works overlook the backhaul network to connect the deployed LiFi APs to the Internet. It means that these systems cannot be used in real IoT applications since their LiFi APs are not actually connected to the Internet. As shown in Table I, wired backhaul solutions for dense battery-free LiFi networks present several difficulties due to the low reconfigurability and flexibility of the network, the extra cost of cabling infrastructure or the cost of dedicated modems. Prior to our LoW-Fi system, there was no work addressing the backhauling problem of LiFi systems with a practical and experimental methodology to target multi-battery-free IoT deployments.

Reverse engineering a WiFi transmitter. The work in [24] does the reverse engineering of Atheros AR2425 chipsets to implement a WiFi to ZigBee physical-level CTC technique. Likewise, OfdmFi [27] emulates a power control per subcarrier to implement a CTC scheme that enables direct communication between WiFi and LTE. In our work, by the first time, we reverse engineer a WiFi transmitter to emulate an M -ASK-OFDM modulation scheme with per subcarrier granularity, and exploit it to implement a WiFi to LiFi cross-technology solution to transmit data to a large number of LiFi APs simultaneously.

VIII. Conclusion

We presented LoW-Fi , a system that targets the problem of designing a bi-directional network architecture suitable for data gathering and processing in battery-free IoT networks. We have extensively evaluated LoW-Fi, and we have shown promising results in terms of reliability and communication range, while providing a scalable solution that uses the subcarriers of a single WiFi channel to provide simultaneous connectivity to the LiFi APs in range of the WiFi router, and also guaranteeing communication in downlink and uplink. Smart homes and offices, Industry 4.0, and smart agri-food facilities (greenhouses and vertical farms), are potential scenarios where our system could be deployed, and we showed its performance in a real smart greenhouse.

REFERENCES

[1] "Everactive. Overcoming the Battery Obstacle, Part I." https://everactive.com/whitepapers/overcoming-the-battery-obstacle-part-i/. Accessed: 2022-10-30.

[2] B. G. Guzman, J. Talavante, D. F. Fonseca, M. S. Mir, D. Giustiniano, K. Obraczka, M. E. Loik, S. Childress, and D. G. Wong, "Toward Sustainable Greenhouses Using Battery-Free LiFi-Enabled Internet of Things," *IEEE Communications Magazine*, vol. 61, no. 5, pp. 129–135, 2023.

[3] M. S. Mir, B. G. Guzman, A. Varshney, and D. Giustiniano, "PassiveLiFi: Rethinking LiFi for Low-Power and Long Range RF Backscatter," in *Proc. of the 27th Annual International Conference on Mobile Computing and Networking*, MobiCom '21, (New York, NY, USA), p. 697–709, ACM, 2021.

[4] M. Hessar, A. Najafi, and S. Gollakota, "NetScatter: Enabling Large-Scale backscatter networks," in *16th USENIX Symposium on Networked Systems Design and Implementation (NSDI 19)*, (Boston, MA), pp. 271–284, USENIX Association, Feb. 2019.

[5] M. Katanbaf, A. Saffari, and J. R. Smith, "Multiscatter: Multistatic backscatter networking for battery-free sensors," in *Proc. of the 19th ACM Conference on Embedded Networked Sensor Systems*, SenSys '21, (New York, NY, USA), p. 69–83, ACM, 2021.

[6] P. Zhang, D. Bharadia, K. Joshi, and S. Katti, "HitchHike: Practical Backscatter Using Commodity WiFi," pp. 259–271, 11 2016.

[7] V. Talla, B. Kellogg, S. Gollakota, and J. R. Smith, "Battery-free cellphone," *Proc. ACM Interact. Mob. Wearable Ubiquitous Technol.*, vol. 1, June 2017.

[8] V. Talla, B. Kellogg, B. Ransford, S. Naderiparizi, S. Gollakota, and J. R. Smith, "Powering the next Billion Devices with Wi-Fi," in *Proc. of the 11th ACM Conference on Emerging Networking Experiments and Technologies*, CoNEXT '15, (New York, NY, USA), ACM, 2015.

[9] D. Ma, G. Lan, M. Hassan, W. Hu, and S. K. Das, "Sensing, Computing, and Communications for Energy Harvesting IoTs: A Survey," *IEEE Communications Surveys & Tutorials*, vol. 22, no. 2, pp. 1222–1250, 2020.

[10] "Jeeva: Reimagining connectivity." https://www.jeevawireless.com/. Accessed: 2022-10-30.

[11] "Haila: Bringing Wi-Fi to IoT." https://www.haila.io/. Accessed: 2022-10-30.

[12] A. Galisteo, A. Varshney, and D. Giustiniano, "Two to tango: Hybrid light and backscatter networks for next billion devices," in *Proc. of the 18th International Conference on Mobile Systems, Applications, and Services*, MobiSys '20, (New York, NY, USA), p. 80–93, ACM, 2020.

[13] "Status of IEEE 802.11 Light Communication TG." https://www.ieee802.org/11/Reports/tgbb_update.htm. Accessed: 2022-10-30.

[14] A. Sturniolo, G. Cossu, A. Messa, and E. Ciaramella, "Ethernet over commercial lighting by a Visible Light Communication," in *2018 Global LIFI Congress (GLC)*, pp. 1–4, 2018.

[15] J. Song, W. Ding, F. Yang, H. Yang, B. Yu, and H. Zhang, "An indoor broadband broadcasting system based on PLC and VLC," *IEEE Transactions on Broadcasting*, vol. 61, no. 2, pp. 299–308, 2015.

[16] W.-D. Zhong, C. Chen, and D. Wu, "Seamless integration of indoor VLC with WDM-PON based on hierarchically modulated constant envelope OFDM," in *2015 17th International Conference on Transparent Optical Networks (ICTON)*, pp. 1–4, 2015.

[17] H. Kazemi, M. Safari, and H. Haas, "A wireless optical backhaul solution for optical attocell networks," *IEEE Transactions on Wireless Communications*, vol. 18, no. 2, pp. 807–823, 2019.

[18] H. Kazemi, M. Safari, and H. Haas, "A wireless backhaul solution using visible light communication for indoor Li-Fi attocell networks," in *2017 IEEE International Conference on Communications (ICC)*, pp. 1–7, 2017.

[19] "G.hn products of MaxLinear for LiFi backhaul." https://www.maxlinear.com/solutions/industrial-multi-market/lifi. Accessed: 2022-10-30.

[20] R. Zhao, F. Zhu, Y. Feng, S. Peng, X. Tian, H. Yu, and X. Wang, "OFDMA-Enabled Wi-Fi Backscatter," in *The 25th Annual International Conference on Mobile Computing and Networking*, MobiCom '19, (New York, NY, USA), ACM, 2019.

[21] A. Galisteo, D. Juara, and D. Giustiniano, "Research in visible light communication systems with OpenVLC1.3," in *Proc. IEEE World Forum on Internet of Things*, pp. 539–544, 2019.

[22] "LoRa Modulation." https://www.semtech.com/lora/what-is-lora. 2022-06-29.

[23] "LoRaSDR." https://github.com/myriadrf/lora-sdr. Accessed: 2022-10-30.

[24] Z. Li and T. He, "WEBee: Physical-Layer Cross-Technology Communication via Emulation," in *Proc. of the 23rd Annual International Conference on Mobile Computing and Networking*, MobiCom '17, (New York, NY, USA), p. 2–14, ACM, 2017.

[25] "Reylux R9 gable frame wide span greenhouse | Sistemas DR." https://www.sistemasdr.es/en/greenhouses/sale-greenhouses-premium-range/reylux-r9-greenhouse-r9/. Accessed: 2023-05-29.

[26] Microchip Technology / Atmel, "ATWINC15x0-MR210xB IEEE 802.11 b/g/n SmartConnect IoT Module." https://www.mouser.es/datasheet/2/268/ATWINC15x0_MR210xB_IEEE_802_11_b_g_n_SmartConnect_-1507285.pdf. Accessed: 2022-10-30.

[27] P. Gawłowicz, A. Zubow, S. Bayhan, and A. Wolisz, "OfdmFi: Enabling Cross-Technology Communication Between LTE-U/LAA and WiFi," *arXiv: 1912.04093*, Dec. 2019.